Scaling studies of percolation phenomena in systems of dimensionality two to seven. II.

Equation of state

Scaling studies of percolation phenomena in systems of dimensionality two to seven: II. Equation of state

Hisao Nakanishi† and H Eugene Stanley

Center for Polymer Studies‡ and Department of Physics, Boston University, Boston, Massachusetts 02215, USA

Abstract. Cluster statistics obtained by the Monte Carlo method for percolation processes in systems of dimensionality two to seven are analysed for the percolation analogue of the thermodynamic equation of state, thus complementing the work of paper I on cluster numbers. In particular, we calculate the scaling functions for the analogues of the thermodynamic potentials and their derivatives, and investigate their dependence on dimension d. We are guided by the two exactly soluble limits of $d = 1$ and the Bethe lattice ($d = \infty$). The scaling region, where a good degree of data collapsing can be observed, is investigated in terms of the two 'thermodynamic' variables, one of which is analogous to the temperature and the other to the magnetic field. This region is found to be comparatively large and symmetrical in two dimensions, but considerably smaller in higher dimensions. In addition, we find that the characteristic forms of the scaling functions are closely related to the 'thermodynamic' stability conditions. Finally, we analyse the logarithmic corrections to the scaled equation of state at the upper marginal dimension, $d_c = 6$, and a numerical demonstration of the significance of the logarithmic corrections is presented in terms of data collapsing.

1. Introduction

The utility of the percolation problem in the framework of critical phenomena has been discussed by many authors (see, for example, the reviews by Stauffer (1979) or Essam (1980)). For example, its possible application to the formation of polymer gels has been treated using various approaches (de Gennes 1979, Coniglio *et al* 1979 and references therein). Another example is the possibility of understanding the peculiar properties of liquid water in terms of correlated percolation (Stanley 1979, Stanley and Teixeira 1980).

Aside from these applications, however, the percolation transition has also been studied for its own sake since its simplicity enables one to probe deeper fundamental features of phase transitions in general. In particular, various scaling hypotheses have been studied (Stauffer 1979 and references therein). While much work has dealt with

the scaling of cluster numbers (Stauffer 1975; see also Stoll and Domb 1978, Leath and Reich 1978, Hoshen *et al* 1979), some discussed the percolation analogue of the thermodynamic equation of state (Essam and Gwilym 1971). The equation of state was first calculated as an expansion in the parameter $(6-d)$ (Stephen 1977; see also Aharony 1980). The first explicit calculations of the equation of state were for the square lattice (Nakanishi and Stanley 1978). This paper extends this work to include higher dimensions, drawing from the same Monte Carlo data as our more recent paper on cluster numbers (Nakanishi and Stanley 1980). We also present qualitative studies of the functional forms of the scaling functions.

This paper is organised as follows. In the remainder of this section, the models of bond and site percolation are introduced and notation is defined. Section 2 considers the relationship between fundamental 'thermodynamic' requirements and the functional dependence of the scaling functions on the scaling variables, following the work of Griffiths (1967) for fluids and ferromagnets. In § 3, we discuss the exactly soluble cases of one dimension and the Bethe lattice, as well as the mean-field solution (Mittag and Stephen 1974) obtained using the analogy to the Potts model (Kasteleyn and Fortuin 1969). In § 4 we present the scaling functions for the square *bond* problem $(d = 2)$, simple cubic *bond* problem $(d = 3)$, and hypercubic *site* problems for $d = 4$–7. Their dimensional dependence is explored with the approach to the mean-field theory in mind. Although both Monte Carlo (Kirkpatrick 1976) and series (Gaunt *et al* 1976) works exist which show some aspects of this trend numerically, neither has considered this problem from the viewpoint of the scaling functions. Section 5 deals with corrections to scaling, while § 6 gives a brief summary.

In bond (site) percolation on a given lattice, each bond (site) is independently occupied with probability p and vacant with probability $q = 1 - p$ while all sites (bonds) are considered occupied. Thus, each realisation of the lattice consists of isolated clusters, each of which is a connected network of sites and bonds. It is this *connectivity* that exhibits critical behaviour in the vicinity of the critical probability p_c. Therefore quantities of interest include the mean number of clusters, G, the probability that a site belongs to an infinitely extending cluster, P, and the mean size of finite clusters.

For the bond problem, Kasteleyn and Fortuin (1969) showed the correspondence to the Q-state Potts model in the limit $Q \to 1$. In this correspondence, the bond probability p and the 'ghost field' h are related to the dimensionless parameters J (exchange integral) and H (external magnetic field) by $1 - p = \exp(-J)$ and $1 - h = \exp(-H)$. The ghost field has an interpretation as the probability that a site is connected to the 'ghost site' via the occupation of a 'ghost bond'. Thus, the introduction of the ghost field serves to make closer the analogy to thermal critical phenomena. The site problem corresponds to a similar but more complicated spin Hamiltonian involving multi-spin interactions (Giri *et al* 1977, Kunz and Wu 1978). In both cases, the percolation analogue of the Gibbs potential of the corresponding spin model is given by the mean number of finite clusters per occupied site,

$$G(\epsilon, h) = (1/p_s) \sum_s' n_s(\epsilon)(1 - h)^s. \tag{1.1}$$

Here $\epsilon \equiv (p_c - p)/p_c$, $p_s = 1$ (for the bond problem) or p (for the site problem), and $n_s(\epsilon)$ is the mean number of s-site clusters per (lattice) site in the absence of the ghost bonds. Only the finite clusters contribute to the sum. Note that, since we use site counting for both bond and site problems, the ghost bonds are coupled to the sites in both cases (Reynolds *et al* 1977). The analogue of the spontaneous magnetisation, the probability

that an occupied site belongs to the infinite cluster†, is given by

$$P(\epsilon, h) = 1 - (1/p_s) \sum_s{}' sn_s(\epsilon)(1-h)^s \tag{1.2}$$

while the analogue of the isothermal susceptibility, the second moment of n_s (which becomes a mean number of sites contained in a finite cluster upon normalisation by $(1-P)$) is given by

$$\chi(\epsilon, h) = (1/p_s) \sum_s{}' s^2 n_s(\epsilon)(1-h)^s. \tag{1.3}$$

The 'thermodynamic' scaling relation tested in our previous work (Nakanishi and Stanley 1978) is stated as follows (Essam and Gwilym 1971): $G(\epsilon, h)$ contains a singular part G_{sing} that is asymptotically a generalised homogeneous function (Hankey and Stanley 1972) in ϵ and h near the critical point $\epsilon = h = 0$. That is, there exist two numbers a_ϵ and a_h such that for all $\lambda > 0$,

$$G_{sing}(\lambda^{a_\epsilon}\epsilon, \lambda^{a_h}h) = \lambda G_{sing}(\epsilon, h). \tag{1.4}$$

An additional assumption was made,

$$G_{sing}^{(1)}(\epsilon, h) \simeq P(\epsilon, h), \tag{1.5}$$

where $G^{(n)}$ indicates the nth partial derivative of G with respect to h. This leads to the following identification of the regular and singular parts of the generating function $G(\epsilon, h)$:

$$G_{reg} \simeq -h + w(\epsilon) \tag{1.6a}$$

$$G_{sing} \simeq G + h - w(\epsilon) \tag{1.6b}$$

where $w(\epsilon)$, a regular function of ϵ only, is approximated by a linear function $w(\epsilon) \simeq a_0 + a_1\epsilon$ for the bond problem on the square lattice. The functional forms

$$G_{sing}^{(n)}(\epsilon, h) = |\epsilon|^{(1-na_h)/a_\epsilon} f_n^{\pm}(h/|\epsilon|^{a_h/a_\epsilon}) \tag{1.7a}$$

$$G_{sing}^{(n)}(\epsilon, h) = h^{(1-na_h)/a_h} g_n(\epsilon/h^{a_\epsilon/a_h}) \tag{1.7b}$$

(where the upper (lower) sign indicates below (above) p_c) were then tested numerically for the square bond problem by Monte Carlo simulation.

The resulting scaling functions are shown schematically in figure 1. The two branches of f_2, f_1 and f_0 approach the same limiting functions as $h/|\epsilon|^{\beta\delta} \to \infty$, and these limits appear to be power-law functions. g_2 shows a rounded maximum near $\epsilon/h^{1/\beta\delta} = 1$ corresponding to $p < p_c$, g_1 is a monotone decreasing function approaching zero as $\epsilon/h^{1/\beta\delta} \to \infty$ with the point of inflection at some positive value of the same variable corresponding to $p < p_c$, and g_0 has a slightly asymmetrical trough with the minimum corresponding to $p < p_c$. A discussion of these points is presented in the next section.

---

† The uniqueness of the infinite cluster has been proved rigorously only for a special class of lattices (Erdös and Rényi 1960) although intuitive arguments exist (Kikuchi 1970). Our Monte Carlo data support the uniqueness for all d considered ($2 \leq d \leq 7$).
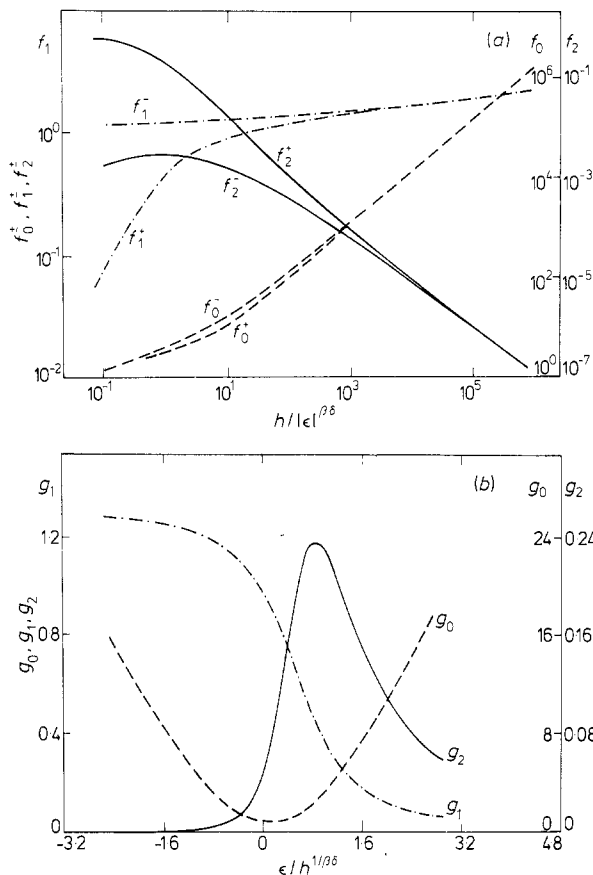
Figure 1. Schematic diagrams of the scaling functions for the $d = 2$ percolation problem. Part (a) plots f_0, f_1 and f_2, each with two branches indicated by $+$ and $-$, while (b) gives g_0, g_1 and g_2.

2. 'Thermodynamics of percolation'

2.1. Percolation–thermodynamics analogies

A close relationship between percolation and the Ising model was already apparent when Sykes and Essam (1963) applied the star–triangle transformation to percolation. This relationship was later made more precise by the exact correspondence to the $Q \to 1$ limit of the Q-state Potts model (Kasteleyn and Fortuin 1969). In this section, we further the analogy by presenting a 'thermodynamic' treatment of percolation following Griffiths (1967). Various percolation quantities are interpreted as analogues of thermodynamic ones, and the thermodynamic requirements for fluids and ferromagnets are translated into the percolation language. This, in turn, leads to some requirements in the forms of the percolation scaling functions.

In a typical Ising ferromagnet near the critical point, the spontaneous magnetisation in zero external magnetic field is shown schematically in figure 2(a). Above the curve, the magnet is homogeneous while below it is inhomogeneous, with ordered 'up' and
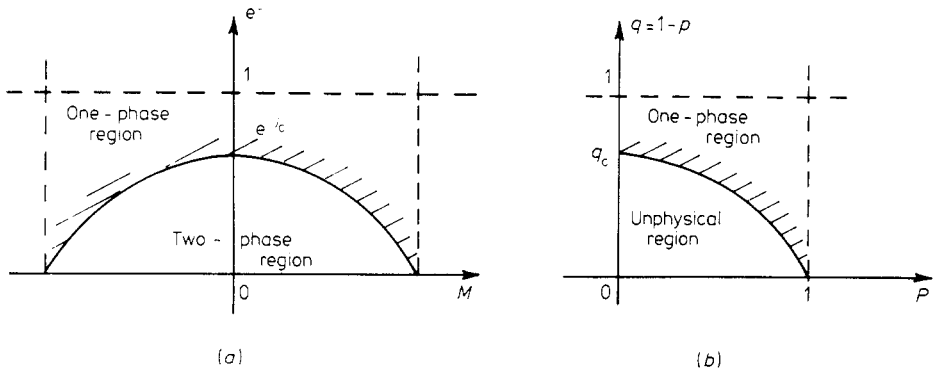
Figure 2. Schematic phase diagrams (a) for a usual Ising ferromagnet where M indicates the normalised spontaneous magnetisation and (b) for the percolation problem with P denoting the percolation probability.

'down' states coexisting. The analogous behaviour of $P(p)$ for the percolation problem is presented in figure $2(b)$.

One important difference is that the order parameter P does not take on negative values, and that the only physical region is the one-phase (or homogeneous) region. Since there is only one kind of ordered state, unlike for an Ising ferromagnet, it is clearly impossible to achieve values of (q, P) falling under the curve in figure $2(b)$. Any point in the one-phase region can be reached by adjusting the value of the ghost field $h = 1 - \exp(-H)$ as in equation (1.2). This situation is illustrated in figure 3.
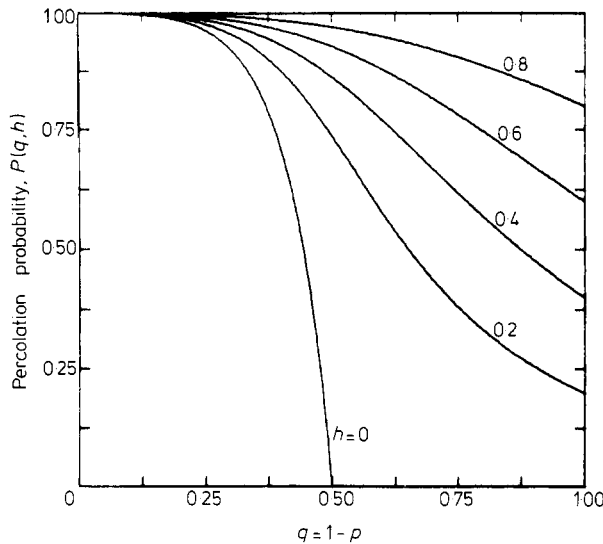

Figure 3. $P(q, h)$ for $h = 0, 0\cdot2, 0\cdot4, \ldots, 0\cdot8$ is plotted for the Bethe lattice of coordination number $z = 3$. The general features remain the same even for the usual lattices.

2.2. Analogues of the thermodynamic potentials

For a simple ferromagnet, the first derivatives with respect to H and T of the Gibbs potential are the magnetisation and entropy. We have already stated that equation

(1.1) gives the percolation analogue of the Gibbs potential. To make the correspondence more direct, however, we define a modified Gibbs potential $\tilde{G}(q, H)$ by

$$\tilde{G}(q, H) = (1/p_s) \sum_s{}' n_s(\epsilon)\,\mathrm{e}^{-Hs} + H \tag{2.1}$$

and its Legendre transform with respect to H is given by

$$\tilde{A}(q, P) = \tilde{G}(q, H) - HP \tag{2.2}$$

where $P = (\partial/\partial H)\tilde{G}$. We note that the second term in equation (2.1) does not change either the analyticity or convexity of G in any way. Clearly we have

$$H = -(\partial/\partial P)_q \tilde{A} \tag{2.3a}$$

$$S = (q\partial/\partial q)_P \tilde{A}, \tag{2.3b}$$

where S is the percolation analogue of entropy. We shall call $\tilde{A}(q, P)$ the 'Helmholtz potential' for percolation since equation (2.3) holds for the Helmholtz potential in the magnetic case[†].

2.3. The Griffiths hypotheses

The six thermodynamic hypotheses of Griffiths (1967) can now be translated into their percolation analogues.

P1: $\tilde{A}$, H, and S exist and are continuous functions of P and q everywhere in the vicinity of the critical point, $P = 0$, $q = q_c$.

P2: On the phase boundary, $H = 0$.

P3: For fixed q, $(\partial/\partial P)^2 \tilde{A}(q, P) \leq 0$, that is, H is a monotone non-decreasing function of P at fixed q.

P4: For fixed P, $(q\partial/\partial q)^2 \tilde{A}(q, P) \geq 0$, that is, S is a monotone non-decreasing function of q at fixed P.

P5: The phase boundary or the percolation curve $q(P)$ is concave near the critical point, and an analytic function of P, except perhaps at $P = 0$.

P6: $\tilde{A}(q, P)$ is an analytic function of both arguments taken together in the vicinity of the critical point except on the phase boundary.

Postulates P1 and P2 are always assumed in the analysis of a second-order phase transition, and they are assumed to hold for percolation also. P3 and P4 correspond, respectively, to the positivity of the mean cluster size (the analogue of the isothermal susceptibility) and the analogue of the specific heat at constant magnetisation. P3 is thus clearly valid, and P4 will be discussed below. P5 and P6[†] are those additional assumptions that do not follow from microscopic thermodynamic principles but are included for aesthetic and empirical reasons.

Let us now discuss the postulate P4. We have an 'entropy'

$$S = (q\partial/\partial q)_P \tilde{A} = (q\partial/\partial q)_H \tilde{G} = (q\partial/\partial q)_H G \tag{2.4}$$

where G is the unmodified Gibbs potential of (1.1). From Kasteleyn and Fortuin

---

† The change in sign in these equations is caused by a negative factor introduced in associating equation (2.1) with the thermal Gibbs potential. This is also responsible for the reversal in some of the convexity properties from the thermal case. The derivative $-\partial/\partial J$ (with dimensionless J) is the thermal analogue of $(q\partial/\partial q)$ in percolation.

‡ If $\ln n_s \sim -s$ for all p below p_c (Klein and Stauffer 1980), P6 is valid on the isochore $h = 0$, $q > q_c$.

(1969), we may interpret S for bond percolation (thus set $p_s = 1$) as

$$S = (q\partial/\partial q)_H G = (\tfrac{1}{2}z)\langle \eta_B \rangle_H \tag{2.5}$$

where z is the coordination number of the lattice, and η_B is 0 if the two terminals of an arbitrarily chosen bond B are connected through occupied bonds, and 1 if not.

For the specific heat, we have

$$C_H = (q\partial/\partial q)_H^2 G = \lim_{N\to\infty}(1/N)\left\langle \sum_{c\neq c'} N_{cc'}^2 \right\rangle_H \tag{2.6}$$

where N is the number of lattice sites and $N_{cc'}$ is the number of bonds that would connect two neighbouring clusters c and c' were they occupied. Kasteleyn and Fortuin (1969) had considered the case where both the lattice and ghost bonds are occupied with the same probability in order to obtain the percolation analogue of Rushbrooke's inequality, while Kirkpatrick (1976) only considered the case $H = 0$; however, it is clearly applicable with H as a fixed, independent parameter as in equation (2.6).

Note that since η_B never takes on a negative value, the entropy S is non-negative and G is non-decreasing in q. In fact, $S = 0$ if and only if either $q = 0$ or $h = 1$ (or $H = \infty$), corresponding to the Ising ferromagnet for $T = 0$ or $H = \infty$ respectively. It is clear that the specific heat at constant external field C_H is non-negative. We can also calculate $(\partial/\partial q)^2 G$ (with no extra factors of q) using the same method, and show that G is convex at fixed H (see figure 4). Clearly, we have $C_H = 0$ for $q = 0$ and for $h = 1$, as well as $C_H = \tfrac{1}{2}z$ for $q = 1$ and $h = 0$. Figure 5 shows $S(q, H_0)$ and $C_H(q, H_0)$ for various values of H_0. We note the disappearance of the broad maximum and the onset of monotonicity of C_H as a function of q with the increase in H. We might summarise this by saying that S gives the degree of non-connectivity of the two nearest-neighbour sites, while C_H is the measure of articulation between pairs of neighbouring clusters.

Postulate P4, however, is the condition of the positivity of the specific heat at constant percolation probability C_P. Consideration of the nature of the ghost-field
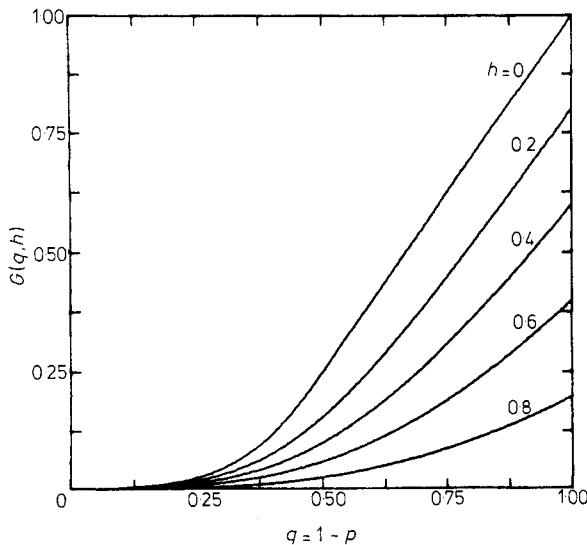
Figure 4. $G(q, h)$ for $h = 0, 0\cdot2, 0\cdot4, \ldots, 0\cdot8$ is plotted for the Bethe lattice of $z = 3$. The general features remain the same for the usual lattices.
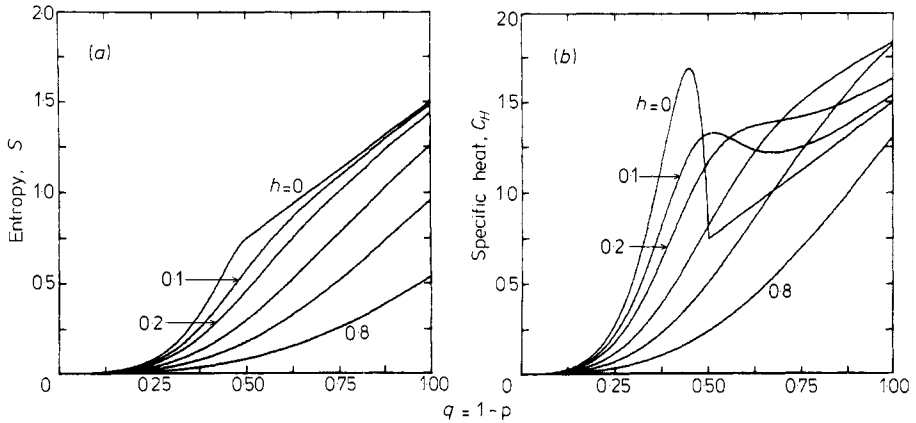
Figure 5. (*a*) Entropy S and (*b*) specific heat C_H for the Bethe lattice of $z = 3$. Note the disappearance of the broad maximum for C_H as h increases.

connectivity reveals that $P = 0 \leftrightarrow H = 0$ for $\epsilon \geq 0$, and therefore

$$\tilde{A}(q, P = 0) = \tilde{G}(q, H = 0) \qquad (\text{for } \epsilon \geq 0) \tag{2.7a}$$

which gives

$$C_{P=0} = C_{H=0} \qquad (\text{for } \epsilon \geq 0). \tag{2.7b}$$

Since we have $C_P \leq C_H$ in general, equation (2.6) is not sufficient to show P4 by itself. However, it does suffice to show that C_P does not diverge to $-\infty$, a catastrophe that could not be rectified by merely adjusting the regular part of the potential.

2.4. Scaling functions

We will now discuss the consequences of these postulates. Following Griffiths (1967), we make a scaling ansatz,

$$H(q, P) = P^\delta \tilde{h}(\epsilon P^{-1/\beta}). \tag{2.8}$$

Then, most of the consequences of P1–P6 are directly analogous to the fluid or ferromagnetic case. As a result of the additional assumption (2.8) (within a finite region of (ϵ, P)) and the discussion presented in appendix 1, we have
   (h1) $\tilde{h}(x)$ is positive, analytic, and $\tilde{h}(-x_0) = 0$;
   (h2) $\tilde{h}(x) = \sum_{n=1}^{\infty} a_n x^{\beta(\delta-n)}$ convergent for $x > R$ with $\tilde{h}(x) \sim x^\gamma$ as $x \to \infty$;
   (h3) $\beta\delta\tilde{h}(x) \geq x\tilde{h}'(x)$;
   (h4) $\tilde{h}''(x) \geq 0$†.
   This leads to a monotone increasing function which is convex and which approaches x^γ asymptotically for large x. For the $d = 3$ simple cubic bond problem, $\tilde{h}(x)$ indeed fits this description including (h4) (figure 6(*a*)), and (h2) is surprisingly well obeyed (figure 6(*b*)). In fact, an analogous plot for the $d = 2$ square bond case (not shown) yields a large region fitting x^γ (with $\gamma = 2.43$) very well.
   Since the scaling functions introduced in § 1 are those derived from $\tilde{G}(q, H)$ rather than $\tilde{A}(q, P)$, we now turn to investigate the relationship between these and $\tilde{h}(x)$. Now,
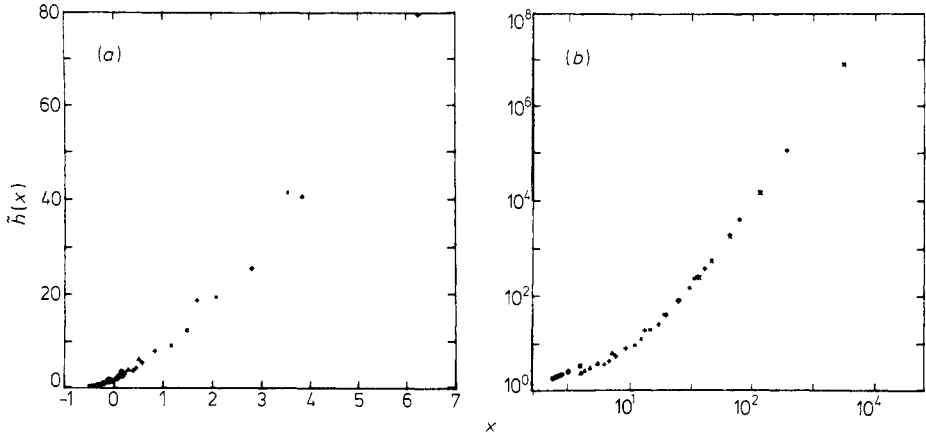
† Not a necessary condition.

Figure 6. Monte Carlo data collapsing for (*a*) the $d = 3$ scaling function $\tilde{h}(x)$ and (*b*) the log–log plot of the same.

we assume in addition

$$P(q, H) = |\epsilon|^\beta \tilde{p}_\pm (H|\epsilon|^{-\beta\delta}) \tag{2.9a}$$

$$= H^{1/\delta} \tilde{p}(\epsilon H^{-1/\beta\delta}) \tag{2.9b}$$

where $\tilde{p}_\pm = f_1^\pm$, and $\tilde{p} = g_1$. Following the discussion in appendix 2, we conclude that:

(p1) $\tilde{p}(-\infty) = +\infty$, $\tilde{p}(\infty) = 0$;

(p2) $\tilde{p}' \leq 0$;

(p3) $\tilde{p}'' \geq 0$ for $x \gg 1$.

For the $d = 3$ simple cubic bond problem, $\tilde{p}(x) = g_1(x)$ indeed fits this description (figure 7). This gives a partial explanation of the functional forms of the scaling functions promised in § 1. The above discussion represents only a minor deviation from the usual
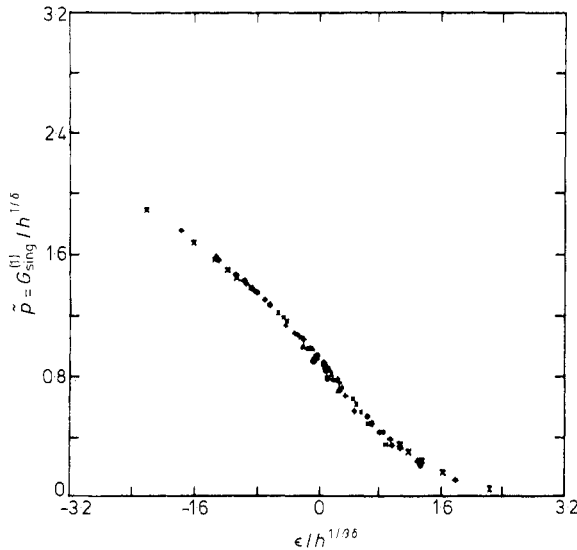

Figure 7. Monte Carlo data collapsing for the $d = 3$ scaling function $\tilde{p}(x)$.

thermal case, and thus we are not surprised to find that the scaling function $\tilde{p}(x)$ is very similar in form to its analogue for the simple ferromagnet (Milošević and Stanley 1972). These characteristics of $g_1(x)$ then lead to those of g_2 and g_0 as described in § 1. The discussion for g_2 and g_0 is presented in appendix 3.

We now turn to the scaling functions obtained by scaling by the other variable (ϵ) depicted in figure 1(*a*). Clearly, scaling functions $f_n^\pm$ and g_n are derivable from each other since

$$\cdot f_n^\pm(x) = g_n(\mathrm{sgn}(\epsilon)x^{-a_\epsilon/a_h})x^{(1-na_h)/a_h} \tag{2.10}$$

where $x = h/|\epsilon|^{a_h/a_\epsilon}$. Therefore

$$f_n^+(x)/f_n^-(x) = g_n(x^{-a_\epsilon/a_h})/g_n(-x^{-a_\epsilon/a_h}). \tag{2.11}$$

The continuity of $g_n(x)$ at $x = 0$, then, implies for all n that

$$f_n^+(x) \sim f_n^-(x) \qquad \text{as } x \to \infty. \tag{2.12}$$

This is precisely what was observed in § 1 since it amounts to the fact that the two branches of f_0, f_1 and f_2 in figure 1 approach one another as the scaling variable grows large. This concludes the qualitative discussion on the forms of various scaling functions.

3. Exactly soluble cases: one dimension and mean-field theory

3.1. One dimension

One of the few exactly soluble systems of percolation is the case of one dimension. Reynolds *et al* (1977) pointed out that the (nearest-neighbour) site and bond problems in one dimension have the same generating function provided that 'zero site clusters' are included in the sum in the case of the site problem. This is correct, but the justification for this procedure comes from the covering transformation which is invertible only for one dimension. For this reason, we prefer to define $G(\epsilon, h)$ by normalising the number of clusters per *occupied* site as described in § 1. To see this, consider the generating function for the $d = 1$ site problem in zero ghost field:

$$G_{\mathrm{site}}(p) = (1/p) \sum_{s=1}^{\infty} q^2 p^s = 1 - p = G_{\mathrm{bond}}(p) \tag{3.1}$$

which is also equal to $\sum_{s=0}^{\infty} q^2 p^s$. If the ghost field is included, then

$$G(\epsilon, h) = (1-p)^2(1-h)/[1-p(1-h)] \tag{3.2}$$

and thus the singular part of $G(\epsilon, h)$ is given by

$$G_{\mathrm{sing}}(\epsilon, h) = (\epsilon^2 + \epsilon h + h^2)/(\epsilon + h). \tag{3.3}$$

The scaling functions $f_0(x_1)$, $g_0(x_2)$ defined in (1.7) are simply

$$f_0(x_1) = (1 + x_1 + x_1^2)/(1 + x_1) \qquad \text{where } x_1 = h/\epsilon, \tag{3.4a}$$

$$g_0(x_2) = (1 + x_2 + x_2^2)/(1 + x_2) \qquad \text{where } x_2 = \epsilon/h. \tag{3.4b}$$

These functions assume an identical form, and are represented by a curve in figure 8. Since in one dimension $\epsilon \ge 0$, f_0 has only one branch. Also shown in figure 8 are f_1, g_1
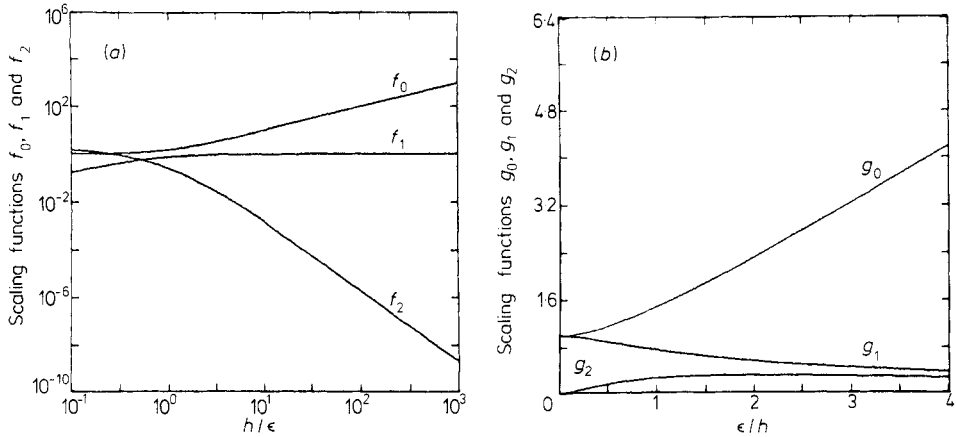
Figure 8. Exact scaling functions for $d = 1$: (a) gives those scaled by ϵ while (b) gives those scaled by h.

(obtained from the first derivative of G_{sing} with respect to h) and f_2, g_2 (from the second derivative). We note that these forms conform to the general features discussed in the previous section.

3.2. Mean-field theory

We now turn to the other closed-form limit, the mean-field theory (MFT), to investigate the general shapes of these curves. In appendix 4, we extend the discussions of Mittag and Stephen (1974) to the case of percolation with the ghost field h (cf Stephen 1977). The resulting Gibbs potential per site (in the $Q \to 1$ limit of the Q-state Potts model) is given by

$$g = 1 + \tfrac{1}{2}zJR^2 - R - (1 - R)\ln(1 - R) + HR \tag{3.5}$$

where z is the coordination number of the lattice and R is the order parameter as defined in appendix 4. We take the derivatives of g with respect to H in order to obtain the percolation analogues of the magnetisation and isothermal susceptibility. For the first derivative,

$$\partial g/\partial H = R + (\partial g/\partial R)(\partial R/\partial H) \simeq (zJ - 1) + [(zJ - 1)^2 + 2H]^{1/2} \tag{3.6}$$

neglecting higher orders. Writing the two scaling fields as

$$x = -zJ + 1 \qquad y = H, \tag{3.7}$$

we arrive at

$$g^{(1)} = -x + (x^2 + 2y)^{1/2}. \tag{3.8}$$

Similarly, for the second derivative,

$$g^{(2)} = (x^2 + 2y)^{-1/2}, \tag{3.9}$$

and for the original Gibbs potential,

$$g = -xy + \tfrac{1}{3}(x^2 + 2y)^{3/2} + w(x). \tag{3.10}$$

We note that $y \simeq h$ and, for large z, $x \simeq (p_c - p)/p_c$, and thus (3.8)–(3.10) are consistent

with the Bethe lattice solution in terms of the critical exponents ($\alpha = -1$, $\beta = \gamma = 1$ and $\delta = 2$).

From (3.10), we obtain for the scaling functions

$$f_0^{\pm}(x_1) = \mp x_1 + \tfrac{1}{3}(1 + 2x_1)^{3/2} \tag{3.11a}$$

$$g_0(x_2) = -x_2 + \tfrac{1}{3}(x_2^2 + 2)^{3/2} \tag{3.11b}$$

where $x_1 = y/x^2$ and $x_2 = x/y^{1/2}$ and the upper (lower) sign corresponds to $x_1 > 0$ ($x_1 < 0$). Similarly, from (3.8),

$$f_1^{\pm}(x_1) = \mp 1 + (1 + 2x_1)^{1/2} \tag{3.12a}$$

$$g_1(x_2) = -x_2 + (x_2^2 + 2)^{1/2}, \tag{3.12b}$$

and from (3.9)

$$f_2^{\pm}(x_1) = (1 + 2x_1)^{-1/2} \tag{3.13a}$$

$$g_2(x_2) = (x_2^2 + 2)^{-1/2}. \tag{3.13b}$$

Figure 9 represents these scaling functions schematically. We note that these diagrams again satisfy the description of § 2, and that only few differences from $d = 1$ (figure 8) or $d = 2$ (figure 1) can be observed. In particular, g_0 now has a minimum for some positive value of x_2, and g_2 is symmetric about the origin.
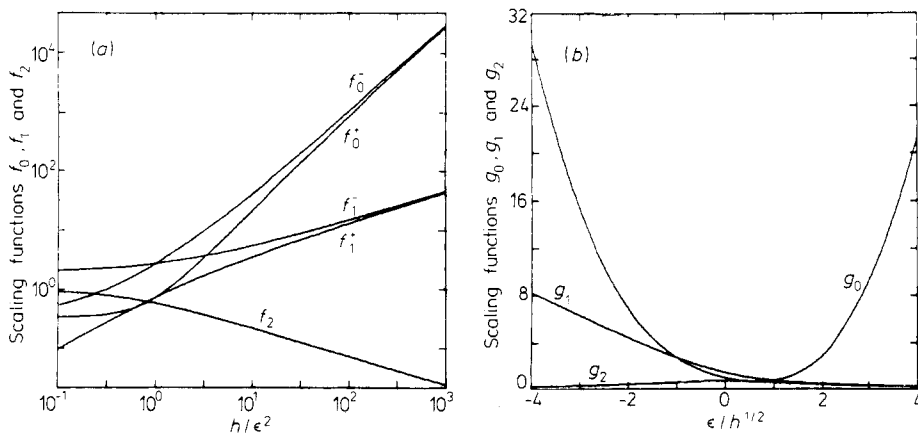
Figure 9. Mean-field scaling functions: (a) scaled by ϵ; (b) by h.

In the percolation limit, the internal energy can be written as $\tfrac{1}{2}zJR^2$ while entropy is given by $(1 - R)(1 - \ln(1 - R))$. A note of caution is that this entropy is defined somewhat differently from that introduced in § 2.

Thus far, we have studied the MFT of the Q-state Potts model to extract information for the percolation problem. Now, however, we calculate the singular parts of the analogues of thermodynamic potentials directly from the known exact solution for n_s on the Bethe lattice. It is instructive to see if there are any substantive differences between these two solutions in terms of the scaling functions.

From § 1, we have

$$G(\epsilon, h) = (1/p_s) \sum_s{}' n_s(\epsilon)(1 - h)^s. \tag{3.14}$$

We shall deal with the bond problem, and thus $p_s = 1$. Here we modify the solution for the site problem (Fisher and Essam 1961; see also Flory 1941, Stockmayer 1943), first because this is a bond problem and second because we include the ghost field h. We find

$$G(\epsilon, h) = \tfrac{1}{2}(1-p)^z(1-h)(2-zX(Z))/(1-X(Z))^z \qquad (3.15)$$

where $z = \sigma + 1$ is the coordination number, $Z(p, h) \equiv p(1-p)^{\sigma-1}(1-h)$ and $X(Z)$ is implicitly determined as that solution of $X(1-X)^{\sigma-1} = Z$ that goes to zero as Z does. Thus, the singular part is given by subtracting from G its regular part,

$$G_{\text{sing}} = G + h - \tfrac{1}{2}(1-1/\sigma) - \tfrac{1}{2}(1+1/\sigma)(1-\sigma p), \qquad (3.16)$$

and the first and second derivatives of G_{sing} with respect to h are

$$G_{\text{sing}}^{(1)} = P = 1 - p(1-p)^{2\sigma}(1-h)^2/[X(Z)(1-X(Z))^{2\sigma}] \qquad (3.17)$$

$$G_{\text{sing}}^{(2)} = [(1-p)^2 Z^2/p]\{2/[X(1-X)^{2\sigma}]$$
$$\qquad - Z[1-(2\sigma+1)X(Z)]/[X^2(1-X)^{3\sigma-1}(1-\sigma X)]\}. \qquad (3.18)$$

Although $X(Z)$ is given only implicitly in general, the case of $z = 3$ ($\sigma = 2$) can be solved explicitly. The scaling functions in this case turn out to be almost identical to those of MFT. For example, we have

$$f_0^{\pm}(x_1) = \mp(3x_1+2) + 2(1+x_1)^{3/2} \qquad (3.19a)$$

and

$$g_0(x_2) = -(3x_2 + 2x_2^3) + 2(x_2^2+1)^{3/2}. \qquad (3.19b)$$

These are substantially the same as (3.11), and the other scaling functions also behave similarly. In particular, the two branches of f_2 collapse into one, and g_2 is symmetric about the origin where the maximum is located. Since the Laplace transform of n_s with respect to s gives the analogue of the Gibbs potential, if the scaling function for n_s is $\exp(-\tfrac{1}{2}x^2)$ (Stephen 1977), then one may expect that the 'thermodynamic' scaling functions contain terms such as $(1 + 2x_1)^{1/2}$ or $(x_2^2 + 2)^{1/2}$. These factors of 2 (as in $2x_1$ or in $+2$) follow from the factor of $\tfrac{1}{2}$ in the exponent in the cluster number scaling function, and are absent for the Bethe lattice solution with $\sigma = 2$ since the n_s scaling function for that case is $\exp(-x^2)$. The factor $\tfrac{1}{2}$ is achieved for the Bethe lattice only in the limit of $z \to \infty$, and thus only then is it entirely equivalent to the MFT solution. With this proviso, the MFT duplicates the more complicated solution for the Bethe lattice. However, the scaled plots of (3.16)–(3.18) (without first taking the scaling limit of $\varepsilon \to 0$, $h \to 0$, and $h/\epsilon^2 \to$ constant) show rather poor data collapsing for $p > p_c$. This may be caused by the special nature of the lattice where there can be an infinite number of infinite clusters above p_c.

4. Monte Carlo results for $2 \leqslant d \leqslant 7$

We have discussed scaling functions $f_n^{\pm}(h/|\epsilon|^{\beta\delta})$ and $g_n(\epsilon/h^{1/\beta\delta})$ which were derived from the nth derivative with respect to h of $G_{\text{sing}}(\epsilon, h)$. Furthermore, figure 1 shows the schematic diagrams of $f_0^{\pm}, f_1^{\pm}, f_2^{\pm}$ and g_0, g_1, g_2 for $d = 2$, while in figures 8 and 9 we do likewise for $d = 1$ and MFT respectively. In this section, we present the scaled plots for $d = 3-7$ (as well as $d = 2$ for comparison purposes) drawing from our extensive Monte Carlo data.

In particular, for $d = 3$, we have generated 12–15 realisations of 100^3 simple cubic bond samples with free boundaries at each of 15 probabilities such that $0 \cdot 2 \leqslant p \leqslant 0 \cdot 3$. Although both p_c and the exponents are varied to test for the best data collapsing visually, the central values employed are $p_c = 0 \cdot 25$, $\beta = 0 \cdot 42$ and $\gamma = 1 \cdot 78$. These are the values obtained as the best estimates based on the same Monte Carlo data previously (cf table IV of Nakanishi and Stanley 1980), and they indeed turn out to be consistent with scaling (figures $10(b)$, $11(b)$, $12(b)$ and $13(b)$). A shift of p_c by as little as $0 \cdot 001$ makes the data collapsing visibly somewhat poorer. Similarly, the series estimates of the exponents (Sykes *et al* 1976a, b) do not produce as good data collapsing. In these plots, the h field ranges from $0 \cdot 005$ to $0 \cdot 025$, which is substantially smaller than the values used to obtain scaling plots for the $d = 2$ square bond problem (Nakanishi and Stanley 1978). If we extend the range to $0 \cdot 1$, we immediately notice the breakdown of data collapsing, at least for $h \geqslant 0 \cdot 04$.

The two branches of the three-dimensional scaling functions $f_2^{\pm}$ are closer together than their counterparts for $d = 2$, implying near symmetry for $p > p_c$ and $p < p_c$ of susceptibility (cf equation (1.3)). In g_2 also the differences are clear between $d = 2$ and $d = 3$: e.g., the maximum value normalised by $g_2(0)$ is much closer to 1 for $d = 3$ than for $d = 2$, although the location is not much different (which is reminiscent of the situation
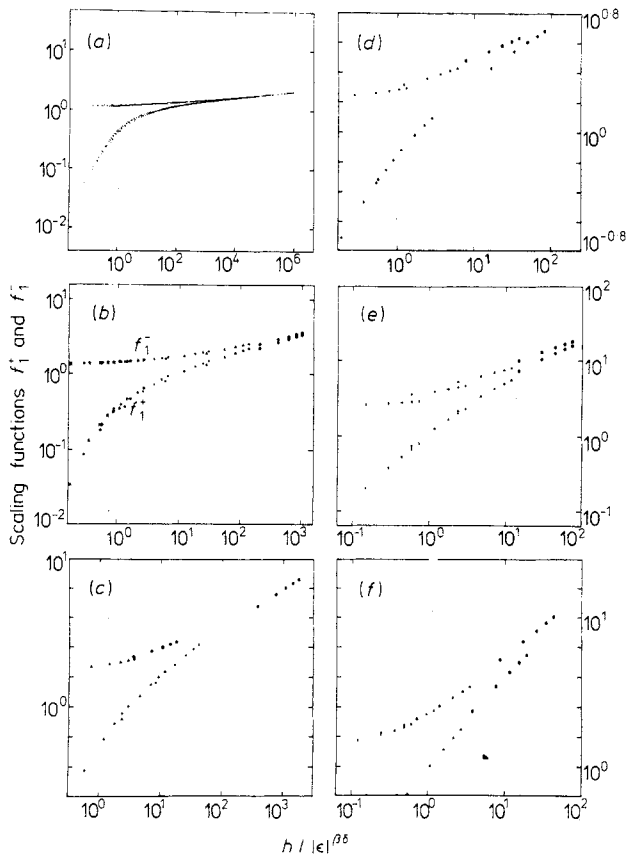

Figure 10. Monte Carlo data collapsing for (a) $d = 2$–(f) $d = 7$ for the scaling function $f_1^{\pm}$. The $d = 6$ data do not include the logarithmic corrections.
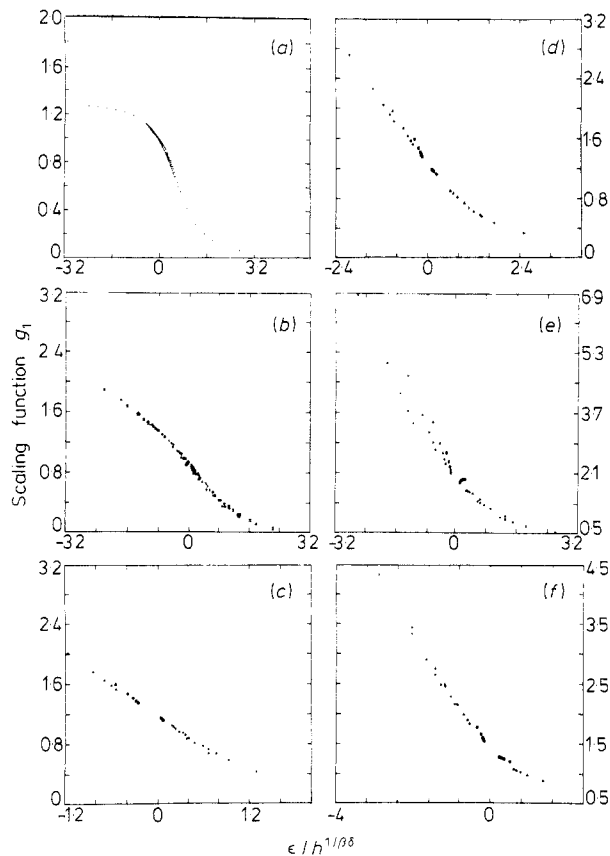
Figure 11. Monte Carlo data collapsing for (a) $d = 2-(f)$ $d = 7$ for the scaling function g_1. The $d = 6$ data do not include the logarithmic corrections.

for the n_s scaling function studied previously). Thus, the $d = 3$ results appear to be visibly closer to the MFT case than $d = 2$ is.

For $d = 4$ and 5, our Monte Carlo data are not as extensive: in these dimensions, 20 realisations of 20^4 ($d = 4$) and 10^5 ($d = 5$) hypercubic site samples are generated with periodic boundaries at each of 6 occupation probabilities: 0·177, 0·187, 0·192, 0·197, 0·207 and 0·217 for $d = 4$, and 0·121, 0·131, 0·141, 0·146, 0·151 and 0·161 for $d = 5$. As in the case of $d = 3$, we have used the best estimates of p_c and the exponents based on our own data as the central values, and varied them to test for sensitivity. These central values are $p_c = 0·198$, $\beta = 0·55$, $\gamma = 1·4$ for $d = 4$, and $p_c = 0·143$, $\beta = 0·60$, $\gamma = 1·3$ for $d = 5$. For $d = 4$, in contrast to the case of $d = 3$, we find that somewhat better data collapsing is achieved with the previous Monte Carlo exponents (Kirkpatrick 1976) of $\beta = 0·52$, $\gamma = 1·6$ still with $p_c = 0·198$, although even with these, the data collapsing is not outstanding, particularly with g_2 (figures 10(c), 11(c), 12(c) and 13(c)). We attribute this mostly to rather large uncertainties associated with our original estimates of the exponents due to the smallness of the samples. For $d = 5$, we still find that our central values are consistent with scaling (figures 10(d), 11(d), 12(d) and 13(d)). However, for both $d = 4$ and $d = 5$, the series estimates (Gaunt *et al* 1976) of p_c and the exponents do not yield as good data collapsing as the Monte Carlo estimates. In all of these plots, h ranges from 0·005 to 0·025.
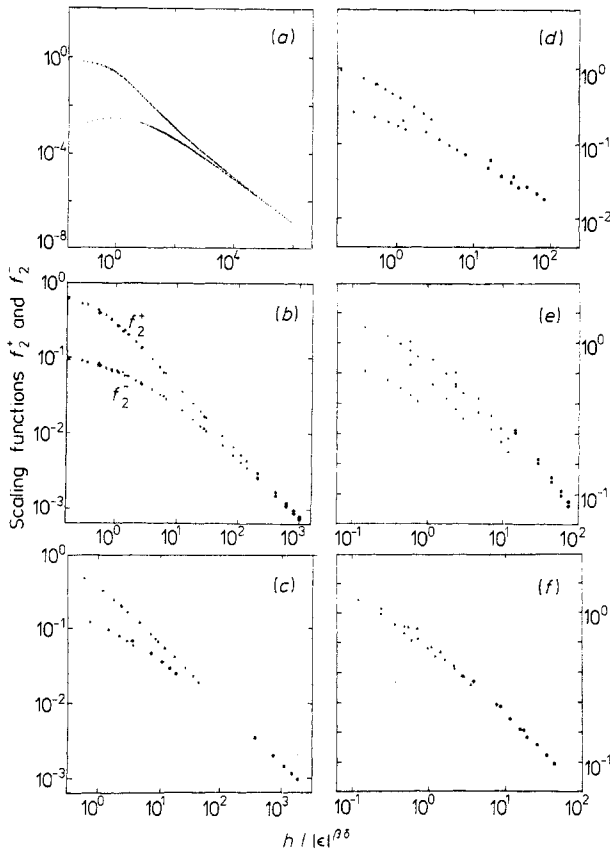
Figure 12. As figure 10, but for the second moment $f_2^{\pm}$.

In comparison with $d = 2$ and 3, we again note the progressive approach of the two branches $f_2^{\pm}$, while in MFT they actually coalesce. Data collapsing is not good for the function g_2, and thus it is hard to estimate either the location or the value of the maximum. However, it does appear that $d = 4$ and 5 continue the trend of $d = 2$ and 3 and the normalised maximum of g_2 decreases further. The concave curvature of g_1 for $\epsilon < 0$ also decreases to approach the overall convexity of the MFT result.

The results for $d = 6$ presented here do not take into account the logarithmic corrections, which will be discussed in the next section. Thus, we use for the exponents the exact values of $\beta = \gamma = 1$. The value of p_c obtained previously for these data was $p_c = 0.108$ (from the susceptibility), which is also the best estimate using series methods (Gaunt *et al* 1976). We have generated 30 samples of 10^6 hypercubic site lattices (with periodic boundaries) at each of 9 probabilities between 0.088 and 0.128. Using the range of h between 0.005 and 0.025, we find both $f_2^{\pm}$ and g_2 not showing a good degree of data collapsing for any reasonable estimates of p_c (figures 10(*e*), 11(*e*), 12(*e*) and 13(*e*)). We find that $f_1^{\pm}$ and g_1 show a comparatively better data collapsing than $f_2^{\pm}$ and g_2 (though not as good as for lower d). We will see in § 5 that this problem can be resolved by including the logarithmic corrections, while $f_2^{\pm}$ do not scale well even with such corrections, presumably due to other correction terms or to a further reduction in the size of the scaling region.
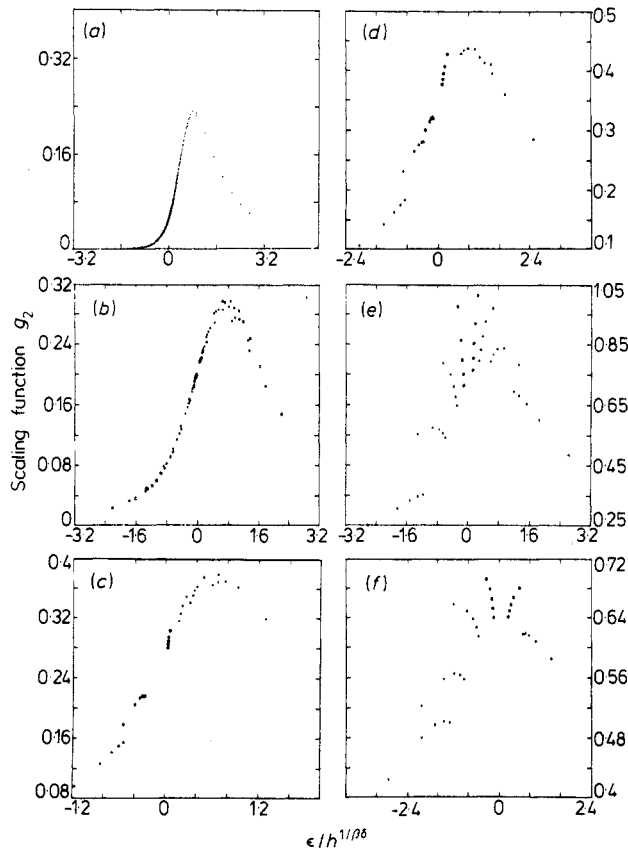
Figure 13. As figure 11, but for the second moment g_2.

Thus, any conclusion we may draw from $f_2^{\pm}$ or g_2 should be taken with a grain of salt. However, it is very likely that the two branches $f_2^{\pm}$ are rather close, as well as that the maximum of g_2 occurs roughly at the origin. In these plots, we present those with the choice of $p_c = 0 \cdot 108$ although without the logarithmic corrections the choice of $p_c = 0 \cdot 106$ appears to scale better.

Our last data are from $d = 7$, where 16 samples of 8^7 hypercubic site lattices (with periodic boundaries) are used at each of 6 occupation probabilities $0 \cdot 075 \le p \le 0 \cdot 1$. Our own estimate of p_c is $0 \cdot 085$ (from susceptibility), and we vary the trial values of p_c for the scaling plots about this value while β and γ are fixed at 1. We find that somewhat better data collapsing is observed with the choice of $p_c = 0 \cdot 083$ than with $0 \cdot 085$, and thus this value is used in figures $10(f)$, $11(f)$, $12(f)$ and $13(f)$ together with $0 \cdot 005 \le h \le 0 \cdot 025$.

It is striking that the two branches $f_2^{\pm}$ now appear virtually collapsed. If this is not an artifact of fluctuations, then $d = 7$ has already the characteristics of the MFT even in the sense that f_2 has only one branch—and thus the susceptibility is symmetric about p_c. The data for g_2 do not appear collapsed, however, and we cannot do more than state that if scaling holds, the maximum ought to be very close to the origin. Moreover, g_1 now seems to be a convex function overall (again similar to the MFT result).

5. Corrections to scaling

Within the framework of the GHF approach, the corrections to scaling can be obtained by including 'irrelevant' parameters in the homogeneity equation. Thus, if μ is such a parameter, we assume (asymptotically for $\epsilon \to 0$, $h \to 0$ and $\mu \to 0$) the generalised homogeneity of the singular part of the mean number of clusters

$$G(\lambda^{a_\epsilon}\epsilon, \lambda^{a_h}h, \lambda^{a_\mu}\mu) = \lambda G(\epsilon, h, \mu) \tag{5.1}$$

for all $\lambda > 0$ provided that all the arguments remain small. This leads to

$$G(\epsilon, h, \mu) = |\epsilon|^{-1/a_\epsilon} G(\pm 1, h/|\epsilon|^{-a_h/a_\epsilon}, \mu|\epsilon|^{-a_\mu/a_\epsilon}) \tag{5.2a}$$

and

$$G(\epsilon, h, \mu) = h^{-1/a_h} G(\epsilon h^{-a_\epsilon/a_h}, 1, \mu h^{-a_\mu/a_h}). \tag{5.2b}$$

From previous work,

$$1/a_\epsilon = 2 - \alpha \qquad 1/a_h = 1 + 1/\delta \qquad a_\epsilon/a_h = \beta\delta. \tag{5.3}$$

When we take for μ the 'most important irrelevant' operator, namely the one with the largest $|a_\mu|$, then the exponent $-da_\mu = \omega$ is termed the correction-to-scaling exponent (Houghton *et al* 1978). In the present case of percolation, μ corresponds to the ϕ^3 operator in the field-theoretic formulation arising from the lack of up–down symmetry in the problem. Unfortunately, however, one does not have a direct way to vary μ, and thus (5.2) cannot be tested directly.

If one expands (5.2) in powers of μ, one recovers the expansion

$$G(\epsilon, h, \mu) = |\epsilon|^{2-\alpha} G_\pm(h|\epsilon|^{-1/\beta\delta}) + |\epsilon|^{2-\alpha+\omega\nu} \mu G'_+(h|\epsilon|^{-1/\beta\delta}) + \dots. \tag{5.4}$$

Taking the case of $h = 0$, one obtains asymptotically

$$G(\epsilon, 0, \mu) \simeq |\epsilon|^{2-\alpha}(A + B|\epsilon|^{\omega\nu}). \tag{5.5a}$$

Similarly, for $p = p_c$,

$$G(0, h, \mu) \simeq h^{1+1/\delta}(A' + B'h^{\omega\nu/\beta\delta}). \tag{5.5b}$$

Thus, corrections to scaling could be tested numerically against the GHF predictions (5.5) provided that $a_\mu < 0$ (or $\omega > 0$), signifying the 'irrelevance' of the parameter μ.

Of course, at the upper critical dimension $d_c = 6$, we have $\omega = 0$, and the approximation made in (5.5) is no longer valid. In fact, the discussions on the logarithmic corrections at $d_c = 4$ of the thermal problem (Wegner and Riedel 1973) turn out to be almost equally applicable for percolation. Thus, the theory predicts logarithmic corrections to scaling (analogous to the thermal problem) which will be described in the remainder of this section.

Wegner and Riedel (1973) showed for the n-vector model with $d = d_c = 4$ that the free energy per spin can be written as

$$\begin{aligned} F(g_1, g_h) = g_0 + \tfrac{1}{2}a'_{011}g_1^2(L + L_0)^{2p+1}/(2p+1) \\ + e^{-4L}\{\delta\mu_0[g_1 e^{2L}(L + L_0)^p] + F(\mu_0 = 0, g_1 e^{2L}(L + L_0)^p, g_h e^{3L})\} \end{aligned} \tag{5.6}$$

where $g_1 \sim t$ (reduced temperature), $g_h \sim H$ (external field) and g_0 is the field corresponding to the constant term in the Hamiltonian. Here, a'_{011} and p are constants which depend on the spin dimensionality. In writing down an expression such as (5.6),

however, one must be cautious, since if one lets the quartic field term go to zero, then the free energy has no lower bound below T_c. This sort of difficulty restricts the applicability of (5.6) so that only the second h-field derivative $F^{(2)}$ makes sense if used directly. The reason for this becomes clear when one considers the mean-field theory, in which the magnetisation $M \sim u^{-1/2}$ ($H = 0$) where u is the ϕ^4 coupling constant.

Thus, we consider for scaling

$$F^{(2)} \simeq e^{2L} F^{(2)}(\mu_0 = 0,\ g_1 e^{2L}(L + L_0)^p,\ g_h e^{3L}). \tag{5.7}$$

In the present case of the Potts model, the last term in (5.6) must be modified as $\exp(-6L)F(\mu_0 = 0,\ g_1 \exp(2L)(L + L_0)^p,\ g_h \exp(4L))$. Thus (5.7) becomes

$$F^{(2)} \simeq e^{2L} F^{(2)}(\mu_0 = 0,\ g_1 e^{2L}(L + L_0)^p,\ g_h e^{4L}). \tag{5.8}$$

This expression together with the vanishing cubic coupling is meaningful, even though there are added complications here because of the existence of the ϕ^3 term in the Potts model Hamiltonian. Setting $|g_1| \exp(2L)(L + L_0)^p = 1$, or $L + L_0 \sim |\ln t|$, we obtain

$$g_h e^{4L} \sim h|t|^{-2}|\ln|t||^{-2p} \tag{5.9a}$$

and

$$F^{(2)} \sim |t|^{-1}|\ln|t||^{-p} r(h/(t^2|\ln|t||^{2p})). \tag{5.9b}$$

Thus, we have a modified form of scaling for χ which incorporates the logarithmic correction. We note $p = -\frac{2}{7}$ for percolation. This particular form (5.9b) is tested using our $d = 6$ data, but the result in a scaled plot (not shown) does not improve data collapsing very much (except for very small h): this should be attributed to other corrections, as well as a small scaling region.

However, if we wanted to find similar logarithmic corrections for the potential itself or the equation of state, we would have to obtain additional information. In the case of the thermal n-vector model, Wegner and Riedel accomplished this by making use of the mean-field theory after taking the system far from criticality by renormalisation with large L. A similar analysis for percolation would thus involve the quartic coupling constant, which must be kept positive for stability and is thus more complicated. We can discuss logarithmic corrections in the following two different ways.

On the one hand, we can write in scaling form the results for the equation of state of Essam *et al* (1978), who used the method of Brézin *et al* (1976) and the calculations of Amit (1976). First, recall the expression for the Q-state Potts model given by Essam *et al*:

$$H(t, R, g, \mu) = [c_1 tR(|\ln R|)^p + c_2 R^2(|\ln R|)^{\frac{1}{4}p - \frac{1}{2}}](1 + \mathrm{O}(1/|\ln R|)). \tag{5.10}$$

Apart from the correction terms, $H(R, t)$ is a generalised homogeneous function with $a_t = a_{\tilde{R}} = \frac{1}{2}$ where $\tilde{R} = R|\ln R|^{-p}$, noting $p = -\frac{2}{7}$ for percolation. This gives

$$H(\epsilon, P) \simeq \epsilon^2 \tilde{f}(P|\ln P|^{-2/7}/|\epsilon|) \tag{5.11a}$$

$$\simeq P^2|\ln P|^{-4/7} \tilde{g}(\epsilon/(P|\ln P|^{-2/7})) \tag{5.11b}$$

where $\tilde{f}$ and $\tilde{g}$ are now explicitly given by

$$\tilde{f}(x) = c_1 x + c_2 x^2 \tag{5.12a}$$

and

$$\tilde{g}(x) = c_1 x + c_2. \tag{5.12b}$$

Equations (5.12) give the global scaling form of the equation of state which contains more information than the logarithmic correction form such as $P \sim |\epsilon| \,||\ln|\epsilon|||^{2/7}$ which is given for $h = 0$ only. Scaling forms (5.11) are tested with our Monte Carlo data, and the scaled plots are presented in figure 14 together with those without the logarithmic corrections. These plots show that the logarithmic corrections (5.11) improve the data collapsing to a considerable degree. The linearity expressed in (5.12b) is also borne out very well. We note also that the form (5.10) is GHF only if $2p = \frac{1}{4}p - \frac{1}{2}$ or $p = -\frac{2}{7}$. This means that in the Q-state Potts model hierarchy, only the percolation limit makes the equation of state with the logarithmic corrections to be a GHF (in modified variables containing logarithms). It is interesting to note that this peculiar property is shared by the Ising model within the n-vector model hierarchy.

On the other hand, the logarithmic corrections for the approaches to the critical point ($\epsilon = h = 0$) along the weak ($H = 0$) and strong ($\epsilon = 0$) paths can be obtained for various 'thermodynamic' functions using the method of Rudnick and Nelson (1976).
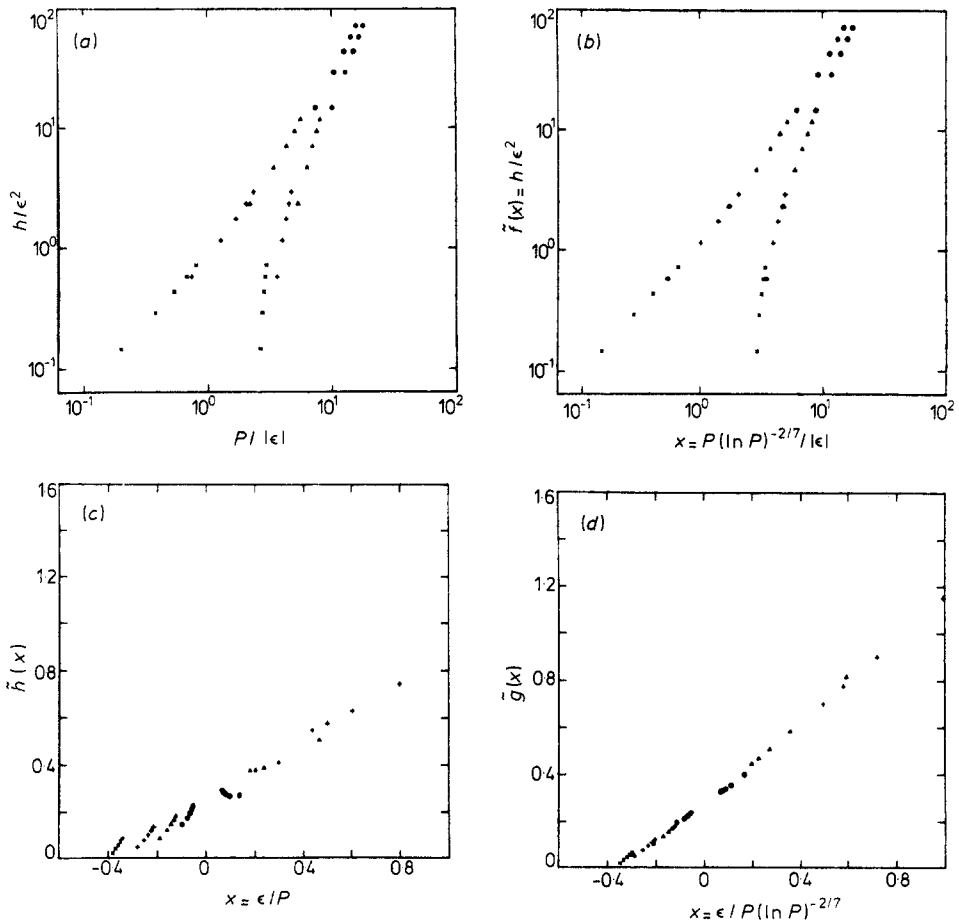

Figure 14. Monte Carlo data collapsing for the logarithmic corrections to the scaled equation of state (cf equation (5.11)). The function $\tilde{f}$ is plotted (a) without and (b) with the logarithmic corrections, and similarly $\tilde{g}$ is plotted (c) without and (d) with the logarithmic corrections.

Since this approach has been illustrated for the function n_s previously, we shall only quote the results here. Let us define θ_1', θ_2', θ_3', θ_1, θ_2, θ_3 by

$$\chi(h = 0) \sim |t|^{-1}|\ln|t||^{\theta_1} \qquad \chi(t = 0) \sim h^{-1/2}|\ln h|^{\theta_1'} \qquad (5.13a)$$

$$R(h = 0) \sim |t||\ln|t||^{\theta_2} \qquad R(t = 0) \sim h^{1/2}|\ln h|^{\theta_2'} \qquad (5.13b)$$

$$G_{\text{sing}}(h = 0) \sim |t|^3|\ln|t||^{\theta_3} \qquad G_{\text{sing}}(t = 0) \sim h^{3/2}|\ln h|^{\theta_3'}. \qquad (5.13c)$$

Then we find that for the Q-state Potts model

$$\theta_1 = -p \qquad \theta_2 = \tfrac{1}{2} + \tfrac{3}{4}p \qquad \theta_3 = 1 + \tfrac{5}{2}p \qquad (5.14a)$$

$$\theta' \equiv \theta_1' = \theta_2' = \theta_3' = \tfrac{1}{4} - \tfrac{1}{8}p \qquad (5.14b)$$

where $p = 2(Q-2)/(10-3Q)$. From (5.14), we immediately see that $\theta_1 = \theta_2 = \theta_3 = \theta' = \tfrac{2}{7}$ for percolation. In fact, all the powers of the logarithmic terms are equal only for $Q = 1$ or the percolation problem. This is a remarkable property since it implies the linear terms in $(6 - d)$ of the exponents γ, $-\beta$, α and $-2/\delta$ are all identical. Of course, it may be said that this cannot be compared with the case for other values of Q since the $(6-d)$ expansions make sense only for small Q $(Q < \tfrac{10}{3})$, but even then it is a notable fact.

In this connection, we must mention that the Ising model occupies a very similar position within the n-vector model. There, the analogues of the exponents θ are $\theta_1 = -p$, $\theta_2 = \tfrac{1}{2}(p+1)$, $\theta_3 = 2p+1$, and $\theta' = \tfrac{1}{3}$ where $p = -(n+2)/(n+8)$. Thus, again, $\theta_1 = \theta_2 = \theta_3 = \theta' = \tfrac{1}{3}$ for $n = 1$ and only for that case. This sort of similarity between the Ising model and percolation has not been noticed before, but it helps to throw light on the special role percolation plays in the hierarchy of the Q-state Potts model.

6. Summary

We have calculated the percolation scaling functions using Monte Carlo simulation for $d = 2-7$, and compared them with the exactly calculable limits of $d = 1$ and the MFT. The general features of these functions thus observed have been interpreted qualitatively from the standpoint of the close analogy to the thermal critical phenomena. This analysis reveals why the percolation scaling functions are so similar in form to those for the usual ferromagnets. Furthermore, we calculated the predictions for logarithmic corrections to the scaling function $\tilde{h}(x)$ at the upper marginal dimensionality, and tested this prediction using our data from $d = 6$. We have observed no qualitative change in the percolation scaling functions at $d = 4$, as in our previous studies of the cluster number scaling (Nakanishi and Stanley 1980).

Acknowledgments

Hoshen. In addition, the Academic Computing Center at Boston University is to be thanked for providing much needed computer time. We also appreciate useful interactions with Drs W Klein, S Muto, S Redner and P J Reynolds.

Appendix 1. Properties of the Griffiths function $\tilde{h}(x)$

In this appendix, we present the discussions leading to (h1)–(h4) of §2. Firstly, it is straightforward to see that P5 implies an inequality $0 \leqslant \beta \leqslant 1$ where $P \sim B(-\epsilon)^{1/\beta}$ for $\epsilon < 0$. In addition, we have:

R1: $\tilde{h}(x)$ is positive, analytic and $h(-x_0) = 0$ where $x \equiv \epsilon P^{-1/\beta}$ and $x_0 = B^{-1/\beta}$;
R1 follows at once from P1, P2, P3 and P6.

For $\epsilon > 0$, by P1 and P6, we have

$$H(q, P) = \sum a_n(\epsilon) P^n \tag{A.1}$$

converging for P less than some $P_0(\epsilon) > 0$. Thus,

$$H(q, P) = \epsilon^{\beta\delta} x^{-\beta\delta} \tilde{h}(x) = \sum a_n \epsilon^{n\beta} x^{-n\beta} \tag{A.2}$$

where the expression on the right converges for sufficiently large x. By noting that $a_n(\epsilon)\epsilon^{\beta(n-\delta)}$ cannot have an ϵ dependence from this, we obtain

$$a_n(\epsilon) = b_n \epsilon^{\beta(\delta-n)}. \tag{A.3}$$

From these considerations,

R2: For some finite constant R, $\tilde{h}(x)$ possesses a series expansion

$$\tilde{h}(x) = \sum_1 b_n x^{\beta(\delta-n)} \tag{A.4}$$

which converges for all x such that $R < x < \infty$. We note that the leading term in equation (A.4) is $x^{\beta(\delta-1)}$ (cf figure 6). In addition, (A.4) implies that $H(q, P)$ is analytic for $P < (\epsilon/R)^\beta$ including the region $P = 0$, $q > q_c$, the region not included by R1.

Since we have

$$(\partial/\partial P)_q H = P^{\delta-1}[\delta\tilde{h}(x) - (1/\beta)x\tilde{h}'(x)], \tag{A.5}$$

P3 gives:

R3: $\beta\delta\tilde{h}(x) \geqslant x\tilde{h}'(x)$ for $-x_0 < x < \infty$.

The consequences of P4 are more difficult to translate to percolation. We start by recalling the definition of the exponent α:

$$C_{H=0} = C_{P=0} \simeq (A/\alpha)(\epsilon^{-\alpha} - 1) + B \qquad (\epsilon > 0). \tag{A.6}$$

We note that $C_{P=0}$ can only be defined for $\epsilon > 0$ since there is no 'two-phase' region in percolation, while $C_{H=0}$ can be defined both below and above p_c. Of course, C_P for general P is defined throughout the 'one-phase' region,

$$C_P = (q\partial/\partial q)_P S = (q\partial/\partial q)_P^2 \tilde{A}. \tag{A.7}$$

The continuity of S (P1) requires $\alpha < 1$, but otherwise there is no *a priori* constraint on the value of α. In fact, we know $-1 \leqslant \alpha < 0$ by numerical methods (see, for example, Stauffer 1979, Essam 1980). Since scaling for $\tilde{A}(q, P)$ near the critical point reads as

$$\tilde{A}(q, P) = A_0(q) + P^{\delta+1} a(\epsilon P^{-1/\beta}), \tag{A.8a}$$

we have

$$C_P \simeq C_0(q) + q^2 P^{-\alpha/\beta} a''(\epsilon P^{-1/\beta}) \tag{A.8b}$$

where A_0, C_0 are analytic functions of q. In fluids and simple ferromagnets, $\alpha > 0$, and therefore the second term would completely dominate in equation (A.8b) near the critical point. This would then mean P4 is valid if and only if $a'' \geq 0$ for all x in the range $-x_0 < x < \infty$. In our case, however, $\alpha < 0$, and thus the condition one can place on a (or $\tilde{h}$) should be much weaker, and at the same time, $C_0(q)$ plays a larger role. For example, if we assume a'' to be bounded, then we must have $C_0(q) \geq 0$. Since $C_0(q) = (q\partial/\partial q)^2 A_0(q)$ where A_0 is the regular part of both $\tilde{A}$ and G, this in turn gives a condition on the regular part of G.

A necessary and sufficient condition for P4 is thus difficult to formulate. However, it is still true that

$$(\partial/\partial P)_q C_P = (q\partial/\partial q)^2_P(\partial/\partial P)_q \tilde{A} = -(q\partial/\partial q)^2_P H. \tag{A.9}$$

Thus, $(x\partial/\partial x)^2 \tilde{h}(x) \geq 0$ would suffice to ensure that C_P is a non-increasing function of P. This would then imply that C_P does not diverge to $-\infty$ as $P \to 0$. Noting that $(q\partial/\partial q) \simeq (q_c\partial/\partial q)$ near q_c,

R4: $\tilde{h}''(x) \geq 0$ for $-x_0 < x < \infty$

is a sufficient condition on $\tilde{h}$ to ensure that the catastrophe of the divergence of C_P to $-\infty$ does not occur. This is clearly much stronger than necessary for this rather loose criterion; however, it might be considered plausible when a much stronger condition P4 is satisfied. These considerations lead to (h1)–(h4).

Appendix 2. Properties of the percolation scaling function $\tilde{p}(x)$

In this appendix, we discuss the characteristics of $\tilde{p}(x)$ based on those of $\tilde{h}(x)$. From (2.9b), we easily obtain

$$\tilde{p}(x) = \tilde{h}(x\tilde{p}(x)^{-1/\beta})^{-1/\delta} \tag{A.10a}$$

$$\tilde{h}(x) = \tilde{p}(x\tilde{h}(x)^{-1/\beta\delta})^{-\delta}. \tag{A.10b}$$

Differentiating equation (A.10b) once, we obtain

$$\tilde{h}'(x) = -\delta\tilde{p}(x\tilde{h}(x)^{-1/\beta\delta})^{-\delta-1}\tilde{h}(x)^{-1/\beta\delta-1}\tilde{p}'(x\tilde{h}(x)^{-1/\beta\delta})[\tilde{h}(x) - x\tilde{h}'(x)/\beta\delta] \tag{A.11}$$

where the quantity in the square brackets is non-negative by R3. Together with $\tilde{h}'(x) > 0$, which follows from (h1) and (h4), this implies

$$\tilde{p}' \leq 0. \tag{A.12}$$

Similarly, $\tilde{h}(-x_0) = 0$ (R1) gives $\tilde{p}(-\infty) = +\infty$, and R2 and equation (A.10b) give $\tilde{p}(+\infty) = 0$ since $\gamma = \beta(\delta - 1) < \beta\delta$ (i.e., $x\tilde{h}(x)^{-1/\beta\delta} \sim x^{1-\gamma/\beta\delta} \gg 1$ for $x \gg 1$).

We now compute $\tilde{p}''$. Noting from (A.10a) that

$$\tilde{p}' = [-(1/\delta)\tilde{h}^{-1/\delta-1}\tilde{h}'][\tilde{p}^{-1/\beta} - (x/\beta)\tilde{p}^{-1/\beta-1}\tilde{p}'], \tag{A.13a}$$

we obtain

$$\tilde{p}' = -(1/\delta)\tilde{h}^{(\alpha-1)/\beta\delta}\tilde{h}'[1 - (x/\beta\delta)\tilde{h}^{1/\beta\delta-1}\tilde{h}']. \tag{A.13b}$$

Using (A.13b) and also the scaling law $\alpha' + \beta(\delta + 1) = 2$,

$$\tilde{p}'' = [1 - (x/\beta\delta)\tilde{h}^{1/\beta\delta - 1}\tilde{h}']^{-3}(-\tilde{h}^{\alpha'/\beta\delta - 1}/\delta)$$
$$\times \{(\alpha'/\beta\delta)\tilde{h}'^2 + \tilde{h}\tilde{h}'' - (x(1-\beta)/(\beta\delta)^2)\tilde{h}^{1/\beta\delta - 1}\tilde{h}'^3\}. \tag{A.14}$$

We note that the quantity in the square brackets can be rewritten as

$$\tilde{h}(y)^{-1}[\tilde{h}(y) - (y/\beta\delta)\tilde{h}'(y)] \qquad y = x\tilde{p}(x)^{-1/\beta}, \tag{A.15}$$

which is non-negative by R3. Thus, the sign of $\tilde{p}''$ is always the opposite of that for the quantity in the curly brackets in (A.14). The sign of this quantity is, however, not trivial to determine. For large x ($\gg 1$), we know $y = x\tilde{p}(x)^{-1/\beta}$ is also large, and $\tilde{h}(y) \sim y^{\gamma}$. Thus, in this limit

$$\{\ldots\} \simeq [(\alpha'\gamma^2/\beta\delta + \gamma(\gamma - 1)) - \gamma^3(1 - \beta)/(\beta\delta)^2]\tilde{h}(y). \tag{A.16}$$

By using the scaling laws, the quantity in square brackets can be rewritten as $-\beta^2\gamma \times (1 + \gamma)/(\beta\delta)^2$, which is negative. Thus, $\tilde{p}''(x) \geq 0$ for $x \gg 1$, as expected from $\tilde{p}' \leq 0$ and that $\tilde{p}(x) \to 0$ as $x \to \infty$. On the other hand, for $x \ll -1$, we have $y \sim -x_0$, and thus $\tilde{h} \sim 0$. If we assume that $\tilde{h}'(-x_0) \neq 0$ (empirically true, cf figure 6), and that $\tilde{h}\tilde{h}'' \to 0$ as $x \to -x_0$, then only the first and last terms can be important in the curly bracket. If $\beta = 1$, as in the MFT, then the last term vanishes, and the expression in curly brackets is negative. On the other hand, if $\beta < 1$, then the second term dominates since $\tilde{h}'$ is bounded, and it is positive. Thus, in particular, the MFT should give $\tilde{p}''(-\infty) \geq 0$. These considerations can be summarised as (p1)–(p3).

Appendix 3. The percolation scaling functions g_2 and g_0

In this appendix, we look into the forms of two other scaling functions, g_2 and g_0 (cf equation (1.7)). By differentiating (2.9b) with respect to H, we obtain

$$(\partial/\partial H)P(q, H) = (1/\beta\delta)H^{1/\delta - 1}(\beta\tilde{p}(x) - x\tilde{p}'(x)) \tag{A.17}$$

which gives

$$g_2(x) = (1/\beta\delta)(\beta\tilde{p}(x) - x\tilde{p}'(x)). \tag{A.17a}$$

Then

$$g_2'(x) = -(1/\beta\delta)[x\tilde{p}''(x) + (1 - \beta)\tilde{p}'(x)]. \tag{A.17b}$$

For the form of $\tilde{p}(x)$ shown in figure 7, $g_2'(x) \leq 0$ for $x \gg 1$. On the other hand, $g_2'(0) = -(1 - \beta)\tilde{p}'(0)/\beta\delta \geq 0$. Thus, $g_2(x)$ has a maximum for some $x \geq 0$. In MFT where $\beta = 1$, this occurs at $x = 0$. This is indeed consistent with the form we saw in § 1.

Recalling equations (1.6) and (1.7), we have

$$(\partial/\partial H)G_{\text{sing}} = (1/\beta\delta)H^{1/\delta}[(2 - \alpha)g_0(x) - xg_0'(x)], \tag{A.18}$$

which gives

$$(2 - \alpha)g_0(x) - xg_0'(x) = \beta\delta\tilde{p}(x) = \beta\delta g_1(x). \tag{A.19}$$

The general solution to (A.19) can be formally expressed as

$$g_0(x) = |x|^{2-\alpha}\left(C - \beta\delta \, \text{sgn}(x) \int^x g_1(t)/|t|^{3-\alpha} \, dt\right) \tag{A.20}$$

where C is to be determined by a suitable boundary condition. Thus, the large-$|x|$ behaviour of g_0 is controlled by the first term, which explains the gross curvature of figure 1. For x very near 0, $\tilde{p}(x)$ can be replaced by $\tilde{p}(0) \simeq 1$, and this gives $g_0(0) \simeq [\beta\delta/(2-\alpha)]\tilde{p}(0) \simeq a_h$. The leading correction, which is given by the linear term in x of $\tilde{p}(x)$, is positive for $x < 0$ while negative for $x > 0$ since $\tilde{p}'(0) < 0$. This last statement explains the 'skewed' appearance of g_0 in figure 1.

Appendix 4. Mean-field treatment of the Q-state Potts model with $Q \rightarrow 1$

Here, we present a mean-field treatment of the Q-state Potts model. We include the external ordering field H, and derive the scaling functions in the percolation limit of $Q \rightarrow 1$ (cf Stephen 1977). We compare these with the exact solution for the Bethe lattice in § 3. Comparisons with the Monte Carlo data for two dimensions up to seven dimensions are made in § 4.

We begin by introducing the problem for $H = 0$. A spin representation introduced by Mittag and Stephen (1974) is used here. In this representation, each state of the Q-state Potts model is represented by a spin variable λ which assumes the value of one of the Qth roots of unity. Then, the dimensionless nearest-neighbour interaction

$$E_{\lambda\lambda'} = -J(\delta_{\lambda\lambda'} - 1/Q) \tag{A.21}$$

can be written as

$$E_{\lambda\lambda'} = (-1/Q)J \sum_{k=1}^{Q-1} \lambda^k \lambda'^{Q-k}. \tag{A.22}$$

Thus, the Hamiltonian for one spin λ in the effective medium of the surrounding spins is given by

$$H_\lambda = (-1/Q)zJ \sum \lambda^k \langle \lambda'^{Q-k} \rangle. \tag{A.23}$$

Here, z is the lattice coordination number and $\langle A \rangle$ denotes the thermal average performed consistently as

$$\langle A \rangle = \text{Tr } A \exp(-H_\lambda)/\text{Tr} \exp(-H_\lambda). \tag{A.24}$$

There are $(Q-1)$ order parameters $\langle \lambda \rangle, \langle \lambda^2 \rangle, \ldots, \langle \lambda^{Q-1} \rangle$ and $(Q-1)$ equations to ensure consistency. To solve for these order parameters, we consider the intuitive physical fact that at low temperatures we expect to have order in which one species is dominant while all the others are equally few. Thus, we have

$$\langle \lambda \rangle = R e^{i\theta}, \tag{A.25}$$

where $e^{i\theta}$ is one of the Qth roots of unity (the dominant species) and R is a real number less than 1. If one further considers $\langle \lambda^m \rangle$, one finds that

$$\langle \lambda^m \rangle = R e^{im\theta} \qquad \text{if } m = 1, 2, \ldots, Q-1 \tag{A.26}$$

since that part of the dominant species giving the modulus R in (A.25) still has the same modulus. The results (A.25) and (A.26) indeed satisfy the consistency requirements (A.24) provided that

$$R e^{i\theta} = \frac{\text{Tr } \lambda \exp[(zJR/Q)(\lambda e^{i(Q-1)\theta} + \ldots + \lambda^{Q-1} e^{i\theta})]}{\text{Tr} \exp[(zJR/Q)(\lambda e^{i(Q-1)\theta} + \ldots + \lambda^{Q-1} e^{i\theta})]}. \tag{A.27}$$

Without loss of generality, let $e^{i\theta} = 1$; that is, consider the root 1 as the dominant species of the phase. Then (A.27) reduces to

$$R = (e^{zJR} - 1)/[e^{zJR} + (Q-1)]. \qquad (A.28)$$

Therefore, the dimensionless internal energy per spin is given by

$$u = (-1/Q)(zJ/2) \sum \langle \lambda^k \rangle \langle \lambda'^{Q-k} \rangle = (1/Q - 1)(zJ/2)R^2 \qquad (A.29)$$

where R is determined by (A.28).

To obtain the dimensionless free energy per spin $-f_Q = -u + s/k_B$, we must calculate the entropy per site s/k_B. From statistical mechanics,

$$s/k_B = -\sum_j n_j \ln n_j \qquad (A.30)$$

where n_j is the expected fraction of spins in the jth state. Let the jth state ($j \neq 1$) be ω^{j-1} where $1 + \omega + \ldots + \omega^{Q-1} = 0$. Then n_j is given by

$$n_j = \langle \delta_{\lambda, \omega^{j-1}} \rangle = (1/Q) \sum^Q \omega^{-(j-1)k} \langle \lambda^k \rangle = (1-R)/Q. \qquad (A.31)$$

Thus

$$s/k_B = -n_1 \ln n_1 - \sum_{j=2}^Q n_j \ln n_j$$

$$= \ln Q - \{[(Q-1)R + 1] \ln[(Q-1)R + 1] + (Q-1)(1-R) \ln(1-R)\}/Q. \qquad (A.32)$$

Combining (A.29) and (A.32), we finally obtain

$$-f_Q = (1 - 1/Q)(zJR^2/2) + \ln Q - \{[(Q-1)R + 1] \ln[(Q-1)R + 1]$$

$$+ (Q-1)(1-R) \ln(1-R)\}/Q. \qquad (A.33)$$

It is clear that this free energy leads to a first-order phase transition for all Q other than 2.

A meaningful limit $Q \to 1$ is obtained from (A.33) by considering the derivative

$$f = (d/dQ)(-f_Q)_{Q=1} = 1 + \tfrac{1}{2}zJR^2 - R - (1-R) \ln(1-R). \qquad (A.34)$$

From the work of Kasteleyn and Fortuin (1969), we know that f corresponds to the mean number of clusters in percolation where the bond probability is given by $p = 1 - \exp(-J)$. The minimum of f is achieved when

$$(\partial/\partial R)f = zJR + \ln(1-R) = 0, \qquad (A.35)$$

and thus the transition is of second order unlike in the original case of (A.33). The critical point is at $zJ_c = 1$ or $p_c = 1 - \exp(-1/z)$, to be compared with the Bethe lattice result of $p_c = 1/(z-1)$ (Fisher and Essam 1961). Also, we note that (A.35) follows if we set $Q = 1$ in the consistency requirement (A.28).

Now let us include a dimensionless field H, that couples to all spins, favouring the species 1. Thus, the dimensionless coupling energy is

$$E_{\lambda H} = -H(\delta_{1,\lambda} - 1/Q). \qquad (A.36)$$

With this addition, the single-spin effective medium Hamiltonian becomes

$$H_\lambda = (-1/Q)zJ \sum^{Q-1} \lambda^k \langle \lambda'^{Q-k} \rangle - (1/Q)H \sum^{Q-1} \lambda^k. \qquad (A.37)$$

Equations (A.24)–(A.26) remain valid, and the consistency condition is now

$$R = (e^{zJR+H} - 1)/[e^{zJR+H} + (Q-1)], \tag{A.38}$$

while the dimensionless Gibbs free energy per spin is given by

$$-g_Q = -f_Q + (1 - 1/Q)HR. \tag{A.39}$$

The percolation limit can be taken, to yield

$$g = (d/dQ)(-g_Q)_{Q=1} = 1 + \tfrac{1}{2}zJR^2 - R - (1-R)\ln(1-R) + HR. \tag{A.40}$$

In analogy to (A.34), g corresponds to the mean number of clusters in percolation where $p = 1 - \exp(-J)$ and $h = 1 - \exp(-H)$ with h (the 'ghost bond' probability) coupling to each site. Its minimum is obtained when

$$(\partial/\partial R)g = zJR + \ln(1-R) + H = 0, \tag{A.41}$$

again the same as (A.38) if $Q = 1$ is substituted. The critical point is unchanged at $zJ_c = 1$, $H = 0$ (or $p_c = 1 - \exp(-1/z)$, $h = 0$).

References

Aharony A 1980 *Phys. Rev.* B **22** 400–14
Amit D J 1976 *J. Phys. A: Math. Gen.* **9** 1441–59
Brézin E, Le Guillou J C and Zinn-Justin J 1976 *Phase Transitions and Critical Phenomena* vol 6, ed. C Domb and M S Green (New York: Academic)
Coniglio A, Stanley H E and Klein W 1979 *Phys. Rev. Lett.* **42** 518–22
Erdös P and Rényi A 1960 *Pub. Math. Inst. Hung. Acad. Sci.* **5** 17
Essam J W 1980 *Rep. Prog. Phys.* **43** 833–912
Essam J W, Gaunt D S and Guttmann A J 1978 *J. Phys. A: Math. Gen.* **11** 1983–90
Essam J W and Gwilym K M 1971 *J. Phys. C: Solid St. Phys.* **4** L228–31
Fisher M E and Essam J W 1961 *J. Math. Phys.* **2** 609–19
Flory P J 1941 *J. Am. Chem. Soc.* **63** 3083, 3091, 3096
Gaunt D S, Sykes M F and Ruskin H 1976 *J. Phys. A: Math. Gen.* **9** 1899–911
de Gennes P G 1979 *Scaling Concepts in Polymer Physics* (Ithaca: Cornell University Press)
Giri M R, Stephen M J and Grest G S 1977 *Phys. Rev.* B **15** 4971–7
Griffiths R B 1967 *Phys. Rev.* **158** 176–87
Hankey A and Stanley H E 1972 *Phys. Rev.* B **6** 3515–42
Hoshen J and Kopelman R 1976 *Phys. Rev.* B **14** 3438–45
Hoshen J, Stauffer D, Bishop G H, Harrison R J and Quinn G P 1979 *J. Phys. A: Math. Gen.* **12** 1285–307
Houghton A, Reeve J S and Wallace D J 1978 *Phys. Rev.* B **17** 2956–64
Kasteleyn P W and Fortuin C M 1969 *J. Phys. Soc. Japan Suppl.* **26** 11–4
Kikuchi R 1970 *J. Chem. Phys.* **53** 2713–8
Kirkpatrick S 1976 *Phys. Rev. Lett.* **36** 69–72
Klein W and Stauffer D 1980 *Phys. Lett.* **78A** 217–8
Kunz H and Wu F Y 1978 *J. Phys. C: Solid St. Phys.* **11** L1–4
Leath P L and Reich G R 1978 *J. Phys. C: Solid St. Phys.* **11** 4017–36
Milošević S and Stanley H E 1972 *Phys. Rev.* B **5** 2526–9
Mittag L and Stephen M J 1974 *J. Phys. A: Math., Nucl. Gen.* **7** L109–12
Nakanishi H and Stanley H E 1978 *J. Phys. A: Math. Gen.* **11** L189–97
—— 1980 *Phys. Rev.* B **22** 2466–88
Reynolds P J, Stanley H E and Klein W 1977 *J. Phys. A: Math. Gen.* **10** L203–9
Rudnick J and Nelson D R 1976 *Phys. Rev.* B **13** 2208–21
Stanley H E 1979 *J. Phys. A: Math. Gen.* **12** L329–37
Stanley H E and Teixeira J 1980 *J. Chem. Phys.* **73** in press

Stauffer D 1975 *Phys. Rev. Lett.* **35** 394–9
—— 1979 *Phys. Rep.* **54** 1–74
Stephen M J 1977 *Phys. Rev.* B **15** 5674–80
Stockmayer W H 1943 *J. Chem. Phys.* **11** 45
Stoll E and Domb C 1978 *J. Phys. A: Math. Gen.* **11** L57–61
Sykes M F and Essam J W 1963 *Phys. Rev. Lett.* **10** 3–4
Sykes M F, Gaunt D S and Essam J W 1976a *J. Phys. A: Math. Gen.* **9** L43–6
Sykes M F, Gaunt D S and Glen M 1976b *J. Phys. A: Math. Gen.* **9** 1705–12
Wegner F J and Riedel E K 1973 *Phys. Rev.* B **7** 248–56